Available online at www.sciencedirect.com
SCIENCE DIRECT®
Journal of Luminescence 111 (2005) 291–305
JOURNAL OF LUMINESCENCE
www.elsevier.com/locate/jlumin

One-, two- and three-photon spectroscopy of π-conjugated dendrimers: cooperative enhancement and coherent domains

M. Drobizhev[a,b], A. Rebane[a,*], Z. Suo[c], C.W. Spangler[c]

[a]*Department of Physics, Montana State University, Bozeman, MT 59717, USA*
[b]*Lebedev Physics Institute, Leninsky pr., 53, 119991 Moscow, Russia*
[c]*Department of Chemistry and Biochemistry, Montana State University, Bozeman, MT 59717, USA*

Available online 24 November 2004

Abstract

We use wavelength tunable femtosecond pulses to measure intrinsic (simultaneous) two-photon absorption (2PA) and three-photon absorption (3PA) molecular cross section in two series of π-conjugated dendrimers built of identical 4,4′-bis(diphenylamino) stilbene (BDPAS) and 4,4′-bis(diphenylamino) distyrylbenzene (BDPADSB) repeat units. Record large 2PA cross sections, $\sigma_2 = 10^{-46}\,\mathrm{cm}^4\,\mathrm{s}$ are obtained for the largest second-generation BDPAS-based dendrimer, as well as zeroth-generation 4-arm BDPADSB-based dendrimer. In both series, maximum 2PA cross section increases nonlinearly with the number of π-electrons, whereas for higher generations this dependence turns to linear one. 3PA cross section also increases nonlinearly with the size of the system in the series of BDPAS-based molecules, amounting a record large value, $\sigma_3 = 10^{-79}\,\mathrm{cm}^6\,\mathrm{s}^2$, for the largest, second-generation dendrimer. We interpret these results in terms of direct inter-branch conjugation, which facilitates cooperative enhancement of the nonlinear-optical response. We propose a simple model which allows us to determine the effective size of coherent domains (extent of conjugation), which, in turn, determines the optimum dendrimer size for most efficient nonlinear response.

PACS: 73.22.−f; 42.50.Hz; 33.80.Wz

1. Introduction

Functional compounds with high efficiency of two-photon absorption (2PA) are indispensable for many innovative photonic applications, such as fluorescence microscopy [1,2], photodynamic therapy [3,4], 3D micro- and nano-fabrication [5,6] and high-density optical data storage [5,7]. Over years, the main design strategy, aiming at enhancing 2PA, has been to construct linear conjugated system with polarizable π bridge, with electron donating and/or electron withdrawing groups attached on both ends [8–10]. Accordingly, a variety of linear structures, including

*Corresponding author. Tel.: +1 406 994 7831; fax: +1 406 994 4452.
E-mail address: rebane@physics.montana.edu (A. Rebane).

0022-2313/$ - see front matter © 2004 Elsevier B.V. All rights reserved.
doi:10.1016/j.jlumin.2004.10.009

bis(diphenylamino)stilbene (BDPAS) [11,12], bis (diphenylamino)distyrylbenzene (BDPADSB) [12,13], and others [8–25], have been investigated in the past in terms of maximizing their 2PA cross section.

Building dendritic molecules as opposed to linear structures appears to be a very attractive alternative, especially because organic dendrimers constructed from optically active units (chromophores) are known to exhibit a whole range of intriguing optical- and spectroscopic properties, including efficient light harvesting [26] and electroluminescence [27]. Furthermore, in comparison to corresponding linear structure or polymer chain, the multi-branched structure of a dendrimer facilitates attachment of various functional groups, as well as provides increased molecular packing density and improved stability performance.

Recently, dendrimers have attracted considerable attention as potential two-photon absorbers for optical limiting in visible- and near-IR range of wavelengths [28–30]. It has been observed that the molecular nonlinear-optical response of branched molecules and dendrimers may increase faster than the number of their constituent subunits, which is an indication of cooperative enhancement [31–37]. However, the actual scaling of nonlinear absorption with dendrimer size (generation) was not systematically studied.

4,4′-bis(diphenylamino) stilbene (BDPAS) and bis(diphenylamino) distyrylbenzene (BDPADSB) are chromophores which are known to exhibit a relatively large 2PA cross section value, especially as compared to their small molecular weight. In this paper, we construct two series of dendrimers built of identical BDPAS and BDPADSB repeat units, and study their intrinsic 2PA and three-photon absorption (3PA) properties. Our choice of base chromophores is motivated by their large intrinsic 2PA cross sections in near-IR [8–14]. Furthermore, in contrast to a majority of optical dendrimers considered so far, our structures are specially designed to facilitate an efficient π-electron delocalization across adjacent dendron arms by using triphenylamino-branching units. As a result, in this paper we are able to demonstrate record large values of intrinsic 2PA and 3PA cross section. What is even more significant, by systematically measuring the scaling of 2PA and 3PA spectra with generation number, we obtain unambiguous experimental proof of a cooperative enhancement effect.

This paper is organized as follows. We start by introducing in Section 2 the fluorescence technique of measurement of 2PA and 3PA spectra, as well as the method of determining the corresponding absolute cross section values. In sections 3.1 and 3.2 we describe the results of 1PA and 2PA spectral measurements, in particular, the nonlinear scaling of maximum 2PA cross section with the number of π-electrons. We find that 1PA and 2PA alone are inadequate to gain sufficient understanding of the microscopic nature of cooperative enhancement of 2PA. As a next step, we show in Section 3.3 that we can get much deeper insight into this effect by using 3PA, which can be described by a transition in simple two-level system. In Section 4, we introduce a simple phenomenological model which allows us to quantify the scaling of 3PA, and also determine the size of coherent domain for each BDPAS-based dendrimer generation.

2. Experimental

The scheme of our experimental setup is shown in Fig. 1. The laser system comprised a Ti:Sapphire femtosecond oscillator (Coherent Mira 900) pumped by 5 W CW frequency-doubled Nd:YAG laser (Coherent Verdi), and 1-kHz repetition rate Ti:sapphire femtosecond regenerative amplifier (CPA-1000, Clark MRX). The wavelength of the oscillator could be tuned in the range 730–820 nm while the amplifier could be operated in the wavelength range 770–800 nm. The amplifier produced 150-fs duration pulses at 0.8 mJ energy per pulse. To extend wavelength tuning, the amplifier output pulses were frequency down-converted using an optical parametric amplifier, OPA (TOPAS, Quantronix). The tuning range of OPA signal beam was from 1100 to 1600 nm, and after frequency doubling in a BBO crystal, from 550 to 800 nm. The OPA output pulse energy was 100–200 μJ (10–50 μJ after

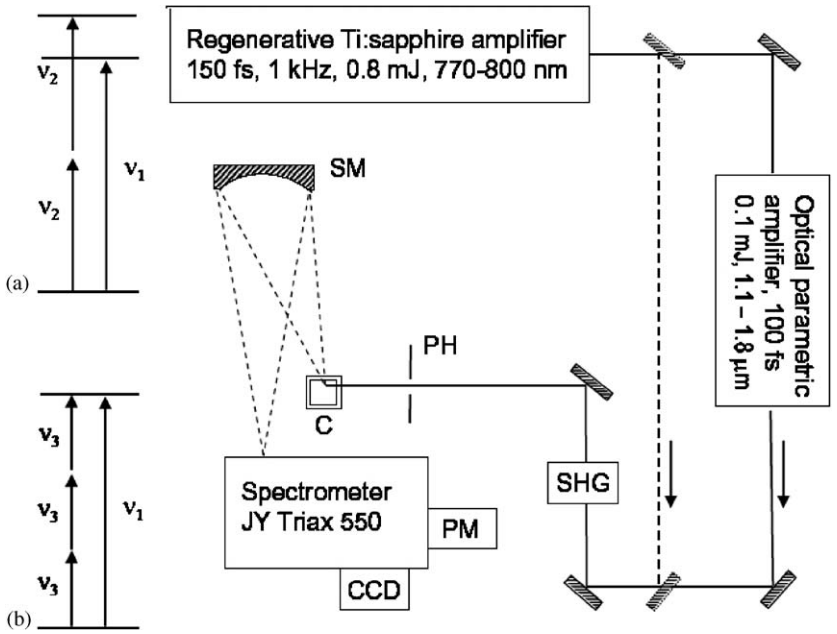

Fig. 1. Schematic of the experimental setup. Frequency ν_2 used in 2PA measurements (a) is either second harmonic of OPA signal beam or is taken directly from the Ti:sapphire system by bypassing the OPA (dashed line). Frequency ν_3 in 3PA measurements (b) is signal beam from OPA. Frequency ν_1 in both types of measurements is second harmonic of Ti:sapphire output. SM, spherical mirror, C, sample cell, PH, pinhole, PM, photomultiplier.

frequency doubling), and pulse duration was 100 fs.

Samples were prepared as dichloromethane solutions at a given molar concentration (10^{-6} M for 1PA and 10^{-5}–10^{-4} M for 2PA and 3PA) and were contained in standard 1 cm spectroscopic cell. A known diameter small pinhole was placed in front of the sample, which guaranteed the ''flat-hat'' beam profile and also the constancy of excitation volume and geometry upon one-, two- and three-photon excitation. The collimated excitation laser beam was passed through the pinhole and directed to the sample. The fluorescence emission was collected with a spherical mirror, and focused on the entrance slit of an imaging grating spectrometer (Jobin Yvon Triax 550).

Linear absorption spectra were measured by standard VIS–UV spectrophotometer (Perkin-Elmer Lambda 900). Nonlinear 2PA spectra were obtained by tuning the wavelength of frequency-doubled OPA output (frequency ν_2, Hz) and measuring the relative intensity of the resulting two-photon excited fluorescence, F_2, while keeping the excitation photon flux and pulse duration constant. Absolute 2PA cross section at one wavelength was obtained by comparing the intensities of two- (F_2) and one-photon (F_1) excited fluorescence measured in the same geometry and setup conditions. The 2PA cross section was then calculated from the following formula (for detailed derivation see [38]):

$$\sigma_2 = \sqrt{\frac{2\pi^3}{\ln 2}} \frac{g\tau r_0^2 h\nu_2^2}{\nu_1} \frac{C_1}{C_2} \frac{F_2}{F_1} \frac{\langle I_1 \rangle}{\langle I_2 \rangle^2} \sigma_1, \quad (1)$$

where g is the laser repetition rate (Hz), τ is the duration of the pulse (FWHM, s), r_0 is the diameter of the pinhole (cm), h is the Plank's constant (J s), C_1 and C_2 are the concentrations (M), $\langle I_1 \rangle$ and $\langle I_2 \rangle$ are the average laser intensities (W) for one- and two-photon excitation, respectively, σ_1 presents a known value of 1PA cross section (cm^2), measured at ν_1. Indexes 1 and 2 in (1) correspond to one- and two-photon excitation

conditions. We used strongly attenuated frequency-doubled output of the Ti:sapphire laser (385–400 nm) as one-photon excitation at frequency ν_1.

3PA spectra were measured in a similar manner by tuning the excitation wavelength, and by measuring the relative intensity of the three-photon excited fluorescence, F_3. The absolute 3PA cross-section was obtained as follows:

$$\sigma_3 = \frac{3\sqrt{3}}{4}\frac{\pi^3}{\ln 2}\frac{g^2\tau^2 r_0^4 h^2 \nu_3^3}{\nu_1}\frac{C_1}{C_3}\frac{F_3}{F_1}\frac{\langle I_1\rangle}{\langle I_3\rangle^3}\sigma_1, \qquad (2)$$

where the designation of symbols is the same as in (1), except that index 3 corresponds to 3PA excitation conditions. This time we used the OPA signal beam directly as the excitation frequency, ν_3, while the frequency-doubled Ti:sapphire around 390 nm still provided the one-photon frequency ν_1.

First, we measured the wavelength dependence of nonlinear absorption, which allowed us to locate the corresponding wavelength of maximum efficiency for 2PA and 3PA. As the second step, absolute cross sections were determined at corresponding spectral maximum, and after that the whole spectrum was normalized to that value.

Fig. 2 shows the chemical structures of two different series of dendrimers studied in this work. The first series comprises the parent 4,4′-bis(diphenylamino)stilbene (BDPAS) molecule, 3-arm zeroth generation dendrimer (3SG0), 4-arm zeroth generation dendrimer (4SG0), first generation (4SG1) and second generation (4SG2) dendrimer with 4-arm core. The synthesis of this series has been described elsewhere [39,40]. Here, we mention that in order to improve solubility of the higher generation dendrimers, we attach *n*-butylthio substituents (SBu) in the para positions of each terminal phenyl ring. The second series comprises BDPADSB parent chromophore and zeroth generation 3-arm (3BG0) and 4-arm (4BG0) dendrimers. Details of the synthesis are described in Ref. [41]. We underline that all studied compounds, including the largest macromolecules, are essentially monodisperse samples.

The quantum chemical calculations were performed with Hyperchem 7 software package. Geometry optimization was accomplished with AM1 method and for spectral calculations we employed the ZINDO/S method.

3. Results and discussion

3.1. Linear spectra

Fig. 3a shows normalized absorption and fluorescence spectra of BDPAS-based series measured under linear (one-photon) excitation conditions. First, we notice that the absorption of all dendrimers is red-shifted with respect to that of the parent molecule. This can be viewed as the first indication that conjugation does increase with the size. However, we also see that after the initial shift to the red, the spectral maximum remains almost the same, up to the highest dendrimer generation. In fact, there is only a slight red shift of the absorption maximum of 4SG2 with respect to 4SG0, whereas 4SG1 is even blue-shifted with respect to both 4SG0 and 4SG2. We have recently performed detailed picosecond time-resolved measurements of fluorescence decay kinetics in this series of dendrimers, and have observed a complex non-exponential behavior, which changes both with the size of the molecule, as well as with the wavelength of emission. We attribute this to several different energy relaxation processes occurring in the excited electronic state, including picosecond energy transfer to more delocalized states [42].

Linear absorption spectra in the BDPADSB-based series (Fig. 3b) are, apart from longer peak wavelength, qualitatively very similar to that of the first series: both zeroth-generation dendrimers show a distinct red shift with respect to the parent molecule, whereas the difference between 3BG0 and 4BG0 is even less than between 3SG0 and 4SG0. In the corresponding fluorescence spectra (not shown) we observe only a small $\sim$100 cm^{-1} increase of the Stokes shift from BDPADSB to 3BG0, while both zeroth generation dendrimers show essentially the same Stokes shift.

Crystallographic data on triphenylamine [43] and BDPAS [44] as well as quantum-mechanical calculations [45] indicate that the three N–C bonds of triphenylamine group in triphenylamine-containing compounds lie in one common plane. Also,

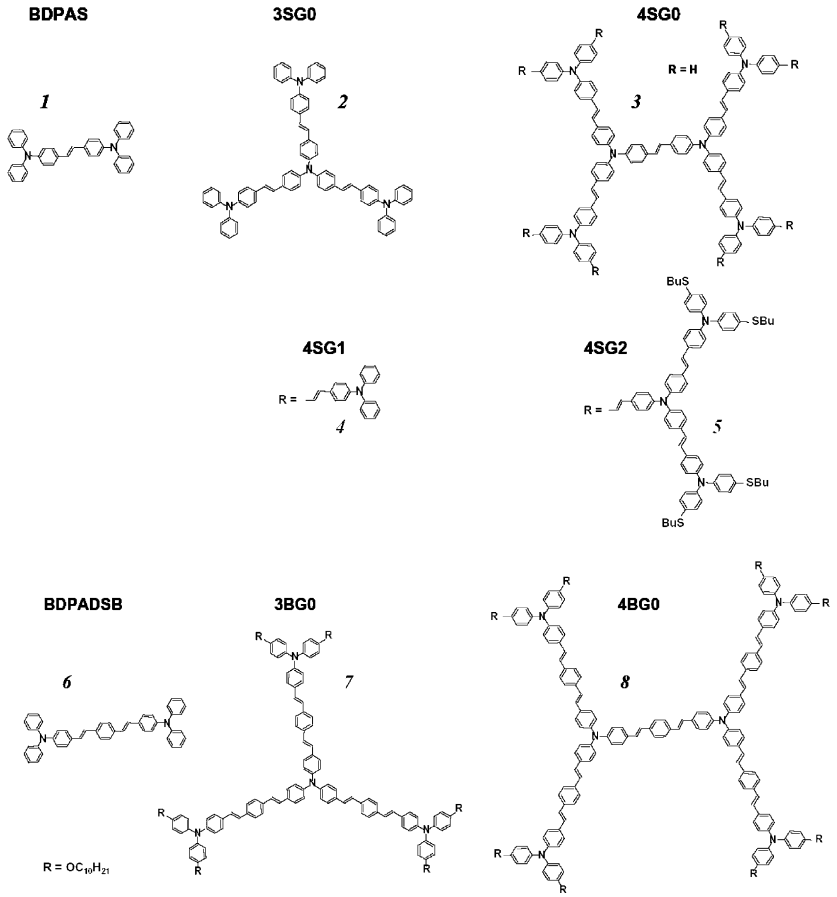

Fig. 2. Molecular structures of the studied compounds. **1**, 4,4′-bis(diphenylamino)stilbene (parent chromophore of BDPAS-based dendrimers); **2**, Three-arm zeroth generation BDPAS-based dendrimer (3SG0); **3**, Four-arm zeroth generation BDPAS-based dendrimer (4SG0); **4**, Four-arm first generation BDPAS-based dendrimer (4SG1); **5**, Four-arm second generation BDPAS-based dendrimer (4SG2); **6**,4,4′-bis(diphenylamino) distirylbenzene (BDPADSB) parent chromophore; **7**, Three-arm zeroth generation BDPADSB-based dendrimer (3BG0); **8**, Four-arm zeroth generation BDPADSB-based dendrimer (4BG0). All these compounds were characterized by high field 1 H and 13C NMR spectra, as well as mass spectrometry. No aggregation effects were observed over a wide concentration range, typically 10^{-4}–10^{-5} M in either polar or nonpolar solvents.

according to crystallographic data [44], in BDPAS two NC_3 planes are parallel to each other. Furthermore, quantum, mechanical calculations and linear optical spectroscopy [45–48] data on triphenylamine and related molecules confirm that the π-conjugation extends all the way through linking nitrogen atoms. Such unusual behavior is credited to the sp^2-hybridization [46–48] of nitrogen, leading to an interaction between the non-paired electron in the nitrogen atom and the π-electrons in the neighbor conjugated units [46–48].

Inserts in Fig. 3 show the dependence of one-photon transition oscillator strength (integrated absorption) on the number of π-electrons, N_π. In both type of structures the oscillator strength is well described by a linear regression. This fact allows us to conclude that, independently of the actual extent or internal structure of conjugation within the dendrimer, the oscillator strength always scales linearly with the overall size of the molecule. Data on the linear absorption properties of all eight compounds are summarized in Table 1.

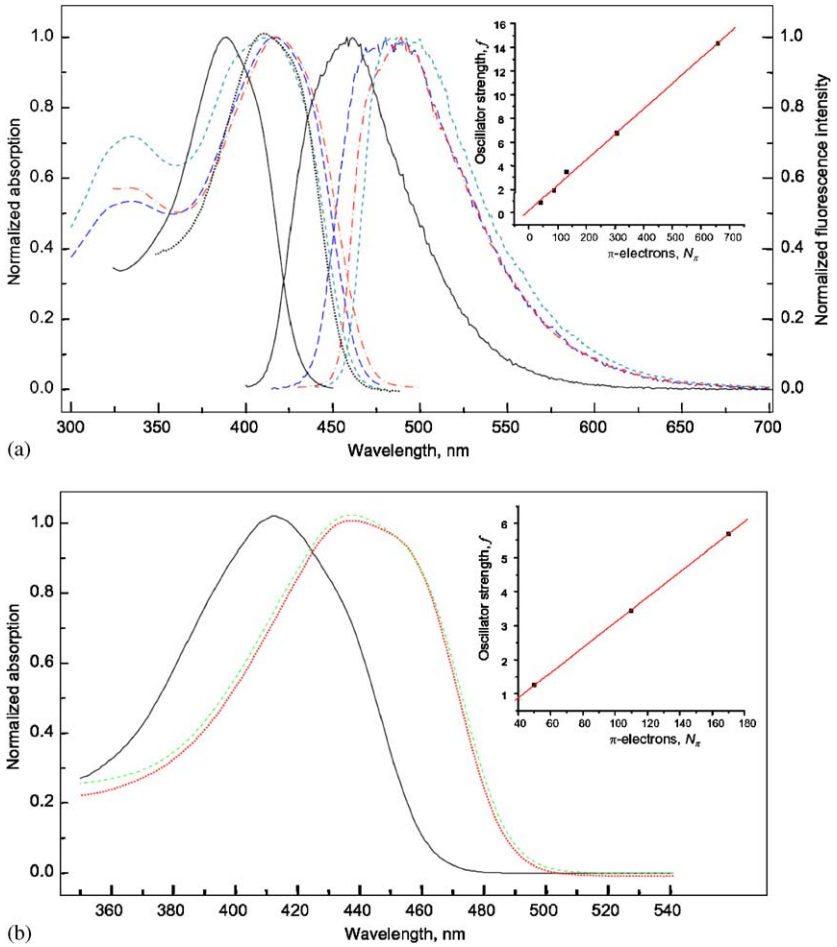

Fig. 3. (a) Linear absorption and fluorescence emission spectra of BDPAS-based dendrimers. BDPAS (solid); 3SG0 (dotted); 4SG0 (long dashed); 4SG1 (dash–dot); 4SG2 (short dashed); (b) Linear absorption spectra of BDPADSB-based dendrimers. BDPADSB (solid); 3BG0 (dotted); 4BG0 (dashed). Inserts show oscillator strength plotted as a function of the number of π-electrons.

Table 1
Summary of 1PA properties of the compounds studied

Molecule	Number of π-electrons, N_π	1PA λ_{max} (nm)	Extinction, ε_{max} ($M^{-1}\,cm^{-1}$)	Oscillator strength, f	f/N_π
BDPAS	42	389	53 000	0.85	0.020
3SG0	86	412	110 000	1.90	0.022
4SG0	130	417	200 000	3.45	0.027
4SG1	306	413	340 000	6.72	0.022
4SG2	658	419	760 000	14.30	0.022
BDPADSB	50	411	90 000	1.26	0.025
3BG0	110	435	230 000	3.43	0.031
4BG0	170	436	370 000	5.69	0.033

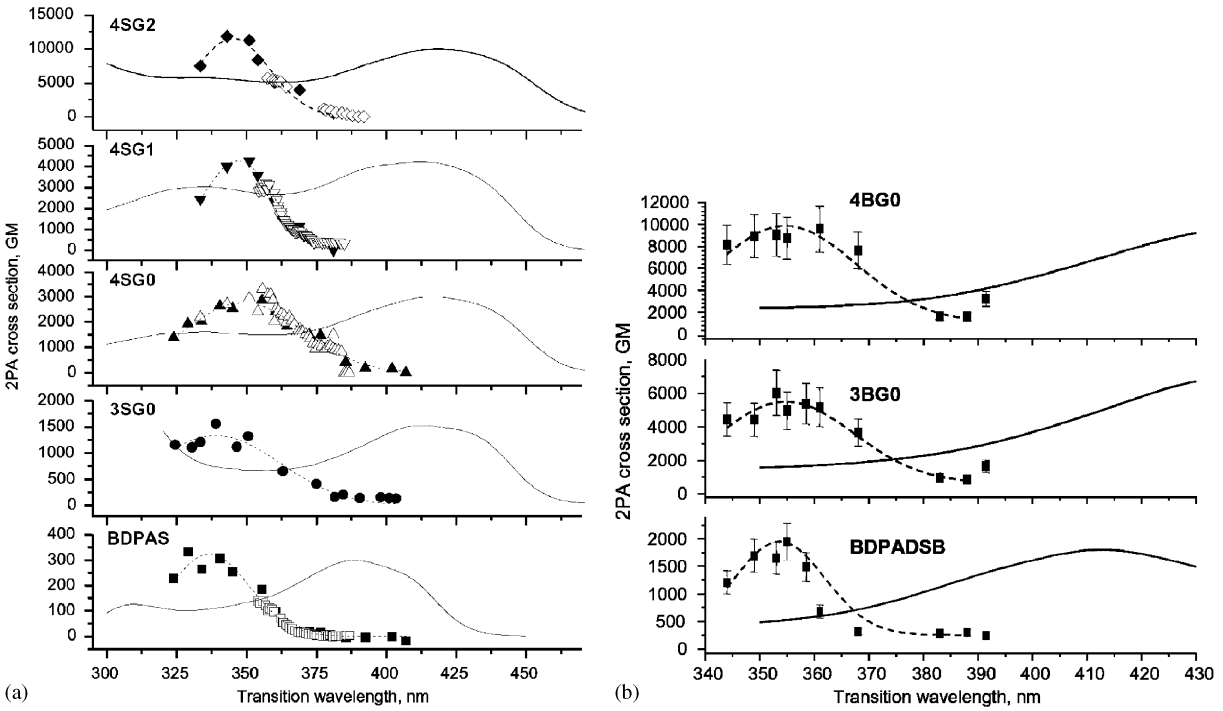

Fig. 4. Absolute 2PA cross section spectra of (a) BDPAS- and (b) BDPADSB-based dendrimers. Filled symbols represent data obtained using SHG of OPA at 1 kHz pulse repetition rate; Empty symbols represent data obtained by using Ti:sapphire oscillator at 76 MHz repetition rate. Dashed curves are Gaussian fits to data points. Solid curves are 1PA spectra.

3.2. Two-photon absorption

Fig. 4 presents the measured cross section as a function of excitation laser wavelength. In all eight compounds, we observe that the 2PA peaks at a transition energy about 4000–5000 cm^{-1} higher than the energy of the lowest one-photon electronic transition. Such marked dissimilarity between the 1PA and 2PA is related to different dipole selection rules that regulate transitions between electronic states of certain parity: for odd number of photons (1PA, 3PA) transitions between opposite parity states are allowed, whereas with even number of photons (2PA) transitions are allowed if the final state has the same parity as the ground state. The 2PA peak has been assigned in both parent compounds to a pure electronic $1A_g \rightarrow 2A_g$ transition [12]. Based on the close similarity between 2PA spectra in Fig. 4, we assume that the rest of the series exhibits the same type of 2PA transition.

Here we mention that, in principle, 1PA and 2PA spectra may peak at different frequencies even if both processes involve the same excited electronic state. This situation occurs especially if the molecule has low symmetry, or if the 2PA transition happens to lend most of its intensity from some high frequency vibronic 1PA transition. In our case, however, this alternative explanation is hardly plausible because of the large value of the observed energy difference.

The 2PA cross section values for all molecules measured in their corresponding maxima are presented in Table 2. The values obtained for the parent compounds, $\sigma_2 = 320$ GM (BDPAS) and $\sigma_2 = 1900$ GM (BDPADSB) are close to those reported earlier [12,13]. All the results communicated here are intrinsic σ_2 values, i.e. those relevant to instantaneous two-photon process. In contrast to our femtosecond fluorescence method, 2PA cross section obtained using longer (nanosecond) pulses and nonlinear absorption methods,

Table 2
Summary of 2PA properties of the compounds studied

Molecule	N_π	2PA λ_{max} (nm)	2PA cross section σ_2, (GM)	$\sigma_2/\sigma_2^{Parent}$	σ_2/N_π (relative values)
BDPAS series					
BDPAS	42	335	320	1.0	1.0
3SG0	86	340	1300	4.1	2.0
4SG0	130	347	2700	8.4	2.8
4SG1	306	347	4500	14	2.0
4SG2	658	345	11,000	34	2.2
BDPADSB series					
BDPADSB	50	353	1900	1.0	1.0
3BG0	110	355	5500	2.9	1.3
4BG0	170	355	9900	5.2	1.5

often tend to considerably exaggerate the value because of large contribution from excited-state absorption [49].

With the above important distinctions in mind, the fact that our dendrimers show very large values, $\sigma_2 = 10^3$–10^4 GM, allows very favorable comparison with known strong two-photon absorbers. In fact, the value $\sigma_2 = 1.1 \times 10^4$ GM of the second generation BDPAS-based dendrimer is, to our knowledge, the largest intrinsic 2PA cross section reported so far for a single molecule [32]. Furthermore, by comparing the cross section of the two dendrimer series, we conclude that by enlarging the conjugation system between the adjacent nitrogen atoms, while maintaining a reasonable degree of planarity, even a low generation dendrimer such as 4BG0 can reach a remarkably large σ_2 value. This effect emerges from the large initial superiority of parent BDPADSB chromophore over parent BDPAS chromophore (6 times larger σ_2), which is explained in its turn, by longer conjugation length or/and an electron accepting ability of the central phenylene ring in the bis(styryl)benzene bridge [8,12]. In practical terms, this means that considerably less synthesis work is needed to produce large 2PA cross section in dendrimers with BDPADSB branches.

The most noteworthy result here is, in our view, not necessarily the maximum or record large 2PA cross section itself, but rather the way this value scales with the size, i.e. generation number of the dendrimer. Fig. 5 presents a double logarithmic

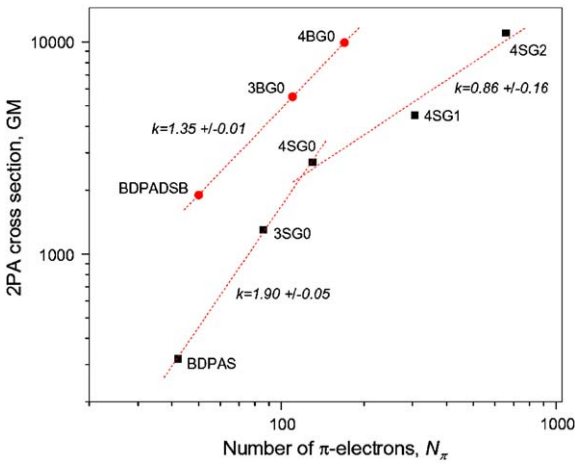

Fig. 5. Dependence of maximum 2PA cross section on dendrimer generation in BDPAS-based dendrimers (circles) and BDPADSB-based dendrimers (triangles). Dashed lines are power law fits.

plot of measured cross section values as a function of the number of π-electrons. While the linear absorption discussed above increased linearly with N_π, one can see that the nonlinear absorption increases markedly faster. In fact, the cross section in the series BDPAS:3SG0:4SG0 scales as 1:4.1:8.4, which is close to the $(N_\pi)^2$-type scaling law, 1:4.2:9.6 (see Table 2). For the second series, BDPADSB:3BG0:4BG0, the 2PA cross section scales as 1:2.9:5.2, which is also faster than the corresponding linear scaling. The fact that the intrinsic nonlinear absorption can increase faster than the size of the system, is generally known as

cooperative enhancement effect, and serves as a key to designing materials with large optical nonlinearity.

In our previous brief communications [32,33,41] we have already reported this effect for BDPAS- and BDPADSB-based dendrimers. In recent paper [34], a faster-than-linear increase of the maximum σ_2 value was also observed in a series of cyano-substituted BDPADSB-type branched molecules. These facts imply that the cooperative enhancement may be a manifestation of a more general property inherent to molecules with a continuous conjugation via nitrogen atoms (so-called *amino conjugation*) [48]. Some other authors [31,36,37] also described nonlinear scaling of σ_2 in multi-branched molecules similar to cooperative enhancement described here. We note, however, that in these earlier reports the 2PA cross section was measured only at one wavelength, which did not allow neither the identification of the shape of nonlinear spectrum, nor the location of the corresponding maximum value. We have seen above that the 2PA spectrum does change, in general, when going from parent molecule to higher dendrimer generations. Therefore, if one is to study a scaling dependence of σ_2, then comprehensive spectral measurements are essential for obtaining quantitatively correct results. For example, the enhancement-type effect observed in Ref. [31] was subsequently explained in terms of (trivial) change in strength of vibronic 2PA transitions [50].

Our next task is to produce a quantitative physical explanation of the experimental results presented above. It is reasonable to limit a sum-over-states expansion to three closest energy levels (three level model), namely, the ground state (index 0), two-photon excited state (f), and one (main) intermediate electronic state (i). Since photon energy is in our case far detuned from the real $0 \rightarrow i$ one-photon transition, and the energies of two photons are the same (degenerate 2PA), then the peak cross section can be expressed as (see, for example, Ref. [8]):

$$\sigma_2 \propto \frac{(E_{f0}/2)^2 M_{i0}^2 M_{fi}^2}{(E_{i0} - E_{f0}/2)^2 \Gamma_{f0}}. \quad (3)$$

Here Γ_{f0} is the linewidth of the two-photon transition, and E_{nm} and $\boldsymbol{M}_{nm}$ are the energy difference and the transition dipole moment between the states n and m, respectively.

Let us first consider the simplest case of a free-electron model of a fully conjugated one-dimensional system [51]. If only one-electron transitions are taken into account, dipole moments $\boldsymbol{M}_{i0}$ and $\boldsymbol{M}_{fi}$ correspond, respectively, to HOMO $\rightarrow$ LUMO and LUMO $\rightarrow$ LUMO + 1 transition. In this case, Eq. (3) gives us readily that the 2PA cross section scales as sixth power of the size of the molecule, $\sigma_2 \propto N_\pi{}^6$. More elaborated quantum-mechanical calculations, which go beyond three-level model and one-electron transition approximation, find for the same one-dimensional π-conjugated systems a power scaling law, $\sigma_2 \propto N_\pi{}^a$, with the exponent value a varying from 2 to 7 [52–54]. It is interesting to note that in Ref. [55] the 2PA cross sections of BDPAS-based dendrimers, considered here were calculated by ZINDO-SOS technique. Although it was not specially emphasized there, the data presented in Table 3 [55] clearly indicate that $\sigma_2 \propto N_\pi{}^2$, which is in a good agreement with our experimental results.

The fact that the power dependence of σ_2 on N_π for amino-conjugated dendrimers is slower than that predicted theoretically in most of the fully conjugated linear systems can imply that either the fragmentation of π-conjugated system in dendrimers starts already from the lowest generations, or these dendrimer generations are still completely conjugated, but the scaling law for fully conjugated branched system deviates from that of linear system. We could in principle distinguish between the two possibilities by directly measuring excited-state transition dipole moment $\boldsymbol{M}_{fi}$ and substituting it into (3) along with all other experimentally evaluated parameters. If the right-hand expression of (3) would scale in the same way as σ_2, we could suggest that the conjugation encounters the entire dendrimer molecule. However, direct experimental determination of $\boldsymbol{M}_{fi}$ is by no means a trivial task, especially if the molecules exhibit fast energy relaxation in the excited state. We have previously reported that the excited state of BDPAS-based dendrimers shows a complicated multi-exponential decay, with some

Table 3
Summary of 3PA parameters of BDPAS-based dendrimers

Molecule	N_π	Calculation (several first singlet–singlet 1PA transitions)				Experiment				
		λ_m (nm)	f_m	$f=\sum_m f_m$	$\sum_m f_m^3/\nu_m^4$	λ (nm)	f	$\sigma_3(10^{-82}\,\mathrm{cm}^6\,\mathrm{s}^2)$ $(\sigma_3/\sigma_3^{\mathrm{Parent}})$	m/m_0	σ_3/N_π (relative values)
BDPAS	42	345	1.45	1.45	1	389	0.85	50 (1)	1	1
3SG0	86	359 358	2.29 1.51	3.80	5.9	412	1.90	1.5×10^2 (3)	1.14 ± 0.11	1.46
4SG0	130	360 353 347	2.18 1.84 2.13	6.15	9.5	417	3.45	4×10^2 (8)	1.32 ± 0.13	2.58
4SG1	306	294 293 289 288 285 281 279 264 254	3.23 0.15 0.43 0.64 2.47 0.30 0.76 0.15 0.12	8.25	8.4	413	6.72	5×10^2 (10)	1.12 ± 0.11	1.37
4SG2	658	—	—	—	—	419	14.3	1×10^3 (20)	1.03 ± 0.10	1.27

N_π is the total number of π-electrons in the molecule, λ_m is the calculated maximum of one-photon transition, f_m is the oscillator strength of the corresponding transition, λ is the wavelength of experimental one-photon peak, f is the corresponding oscillator strength, σ_3 is the absolute 3PA cross section in maximum, m/m_0 is the relative size of average coherent domain in the dendrimer. Experimental error of relative σ_3 values is 20%. This presents a main contribution to an experimental error of m/m_0, which is estimated to be $\sim$10% by using the square root dependence of m/m_0 on $\sigma_3/\sigma_{3,0}$ (7). The value σ_3/N_π (last column) represents a 3PA enhancement factor, relative to BDPAS.

dynamics taking place on picosecond time scale [42]. Even if we could measure transient excited state absorption, then establishing viable quantitative value for $\boldsymbol{M}_{fi}$, which is relevant to formula (3), will still be less than straightforward.

3.3. Three-photon absorption in BDPAS-based dendrimers

From the previous section it is obvious that the coherent interaction of π-electrons is playing a decisive role in nonlinear optical properties of dendrimers. Given the experimental evidence presented above, in particular, the fact that 2PA cross section starts out with an N_π^a $(a>1)$ type scaling for smaller dendrimers, which then reverts to linear dependence for larger dendrimers, we can state that, at least for large generations, conjugation length has a certain limit, which cannot be exceeded starting from a certain molecular size. The explanation of this fact appears to be obvious especially if we take into account that the large dendrimer generations are likely to lose their planarity and turn into a more globular structure, which is a known inhibitor of extended conjugation. As a dendrimer grows larger, we expect the conjugation to break up into smaller subunits or domains (coherence domains). Therefore, our next task here will be to reveal the existence of such coherence domains, and determine, if possible, their number and size. Besides presenting a fundamental interest, the quantitative knowledge of the origin of the extended conjugation, in particular, the properties of coherence domains is crucial for design of macromolecules with optimized nonlinear-optical response [56]. Up to this point, available experimental data give only a qualitative picture of cooperative enhancement. As described above, 1PA alone cannot provide useful information on coherence domain size, especially if the bathochromic shift of absorption maximum is of the order of spectral band width. 2PA data, while qualitatively suggesting the effect of cooperativity, are not so transparent for the quantitative treatment.

One possibility to achieve better quantitative understanding of these processes is to supplement the experimental data by performing measurements of simultaneous 3PA. There are two important advantages that make 3PA, at least under current circumstances, a very attractive and useful spectroscopic tool. First, because 3PA obeys the same parity selection rules as 1PA, we can expect that the 3PA transition will occur into the same excited electronic state (more specifically for our case, the lowest excited singlet state) as the corresponding 1PA transition. As we will show below, this property will greatly simplify the analysis of cooperative enhancement by essentially eliminating the higher-lying excited states. Secondly, because 3PA is a fifth-order nonlinear-optical effect, and transition dipole moments enter into the corresponding cross section value expression as higher-order power function, the corresponding scaling behavior is even more sensitive to the cooperative effects than in the case of 2PA.

Fig. 6 presents the measured 3PA spectra, along with the corresponding linear (one-photon) absorption spectra in the region of the lowest 1PA band, for the parent BDPAS molecule and the largest 4SG2 dendrimer. The lower wavelength scale shows the 1PA transition wavelength, which corresponds to one-third of the 3PA illumination wavelength (upper scale). It is evident that the 3PA spectrum generally follows the profile of the 1PA spectrum, and that maxima of both spectra virtually coincide. This is not surprising because, independently of molecular symmetry, 1PA and 3PA obey the same parity selection rules. This behavior also corroborates our earlier observation that there are no two-photon-allowed levels in a gap below the depicted absorption band. Otherwise, the 3PA spectrum would be shifted due to the 2PA intermediate resonance. The high value of the quantum yield of fluorescence [32], along with the results of our quantum-mechanical calculations, presented below, serve as a further support that there are no any intermediate dark singlet states in the series of dendrimers under study.

With this information in hand, we measured σ_3 for each molecule at an excitation wavelength, corresponding to 3PA maximum wavelength. The results are presented in Table 3.

Comparison with previous literature data [57–60] shows that already BDPAS molecule has

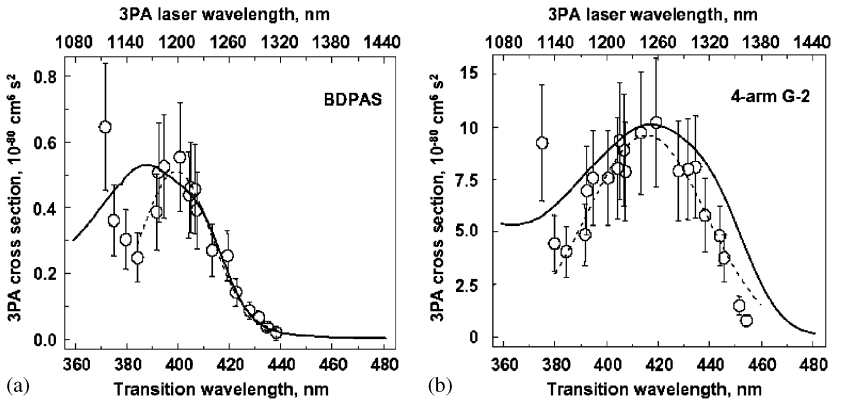

Fig. 6. Absolute three-photon spectra of BDPAS parent and 4SG2 dendrimer in dichloromethane. Dashed curves—Gaussian fits to 3PA bands. Solid curves—one-photon absorption spectra. The abscissa shows transition wavelength, which is one-third of excitation laser wavelength in case of 3PA.

a particularly large σ_3 value. With the increase of the dendrimer size, we observe a drastic increase of σ_3. For 4SG2 molecule, $\sigma_3 = 10^{-79}\,\mathrm{cm}^6\,\mathrm{s}^2$, which is, to our best knowledge, one of the largest values measured so far for any organic molecule by fluorescence technique. We estimate that our error (standard deviation) in the absolute σ_3 measurement is about 30%, and the error of relative σ_3 values (with respect to BDPAS) in the whole series is 20%.

We now turn to the analysis of the scaling behavior of the spectral maximum value of σ_3 in the series of dendrimers. Fig. 7 presents a double-logarithmic plot of this value versus N_π. One can see that σ_3 scales according to power law, $\sigma_3 \propto N_\pi^a$ with $a = 1.7 \pm 0.2$, when going from parent (BDPAS) to 4SG0 dendrimer, and then levels off showing saturation at higher generations. The higher-than-linear power law at lower generations implies again that there exists an inter-branch coupling, at least up to G-0 generation.

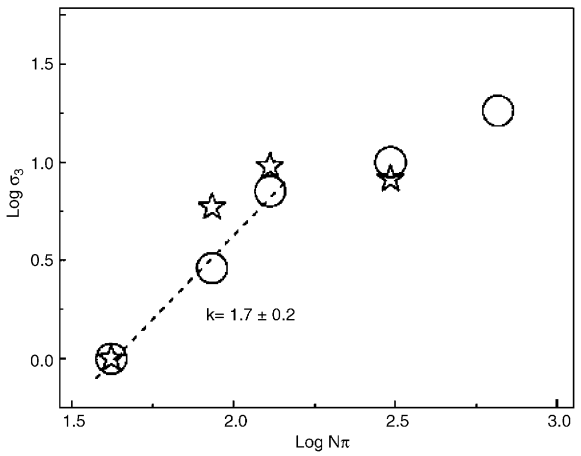

Fig. 7. Double logarithmic plot of relative 3PA cross section versus the number of π-electrons in molecule; circles—experiment, stars—quantum chemical calculations. For the first three molecules the scaling law is nonlinear (dashed line has a slope 1.7).

3.4. Model of coherent domains and scaling of 3PA

Our model of coherent domains in a dendrimer is as follows. Assume that a dendrimer comprises a number μ uncoupled domains, each of which contains (on average) m coherently coupled π-electrons ($N_\pi = \mu\ m$). Assume also that BDPAS contains only one such domain with m_0 coherently coupled electrons. Since we observe that the overall oscillator strength scales linearly with the number of π-electrons, $f \propto N_\pi$, we can conclude that inside each domain, possessing oscillator strength f_m, this latter value also scales linearly with the number of π-electrons:

$$f_m \propto m. \tag{4}$$

As a result, we can write for the total number of π-electrons in a dendrimer:

$$\mu m \propto f. \tag{5}$$

Since we observe no intermediate states between the ground and final levels, then, along with high oscillator strength value, $f_m \sim 1$, using simple two-level model for describing the 3PA within each domain appears to be well justified. Under these conditions, one obtains a simple expression for maximum 3PA cross section within each coherent domain [58],

$$\sigma_{3,m} \propto \frac{f_m^3}{\nu_m^4} g_m(0), \tag{6}$$

where ν_m, and $g_m(0)$ are the central frequency and normalized spectral shape function in the maximum of the corresponding three-photon transition within mth domain. Then, the total 3PA cross section per dendrimer will be,

$$\sigma_3 \propto \sum_m \frac{f_m^3}{\nu_m^4} g_m(0). \tag{7}$$

In order to double check the validity of two-level approximation, and of the basic for our model Eq. (7), we carried out quantum-mechanical calculations of 1PA spectra of all the molecules studied here, up to 4SG1. The corresponding wavelengths and oscillator strengths are presented in Table 3. The main qualitative result of these calculations is that, whereas in BDPAS the first S_0–S_1 electronic transition is well isolated from the others and polarized along the N–N stilbene axis, in all other molecules this transition is split into a number of close-lying transitions, with different polarizations. We assign these transitions to absorption in decoupled coherent domains, discussed above. The number of these transitions (multiplicity of splitting) increases with the size of molecule. Quantitatively, we have calculated the value $\sum_m f_m^3/\nu_m^4$ (we assume here $g(0)$ to be constant) for all the molecules relatively to BDPAS and presented it in Table 3 and in Fig. 7. A reasonably good correlation between the relative values of calculated $\sum_m f_m^3/\nu_m^4$ and experimental σ_3 serves as a confirmation of our model (Eq. (7)).

Because our model implies that all domains are of equal size, it is reasonable to suggest that $\nu_m = \nu$, and $g_m(0) = g(0)$ are the same for each domain. Then the equation (7) yields,

$$\sigma_3 \propto \frac{g(0)}{\nu^4} \sum_m f_m^3 = \frac{g(0)\mu f_m^3}{\nu^4}. \tag{8}$$

By using (4), we get,

$$\mu m^3 \propto \frac{\nu^4 \sigma_3}{g(0)}. \tag{9}$$

Now we can estimate the size of coherent domains, relatively, for example, to BDPAS, in each dendrimer by solving the system of Eqs. (5) and (9):

$$\frac{m}{m_0} = \left(\frac{\nu}{\nu_0}\right)^2 \sqrt{\frac{\sigma_3}{\sigma_{3,0}} \frac{f_0}{f} \frac{g_0(0)}{g(0)}}, \tag{10}$$

where index 0 corresponds to the values obtained for BDPAS.

Here we will use the nonlinear scaling of σ_3 to estimate the size of effective coherence domain (conjugation length) in each dendrimer of BDPAS-based series. Experimentally we observe only very little (less than 5%) variation in $\nu^2/[g(0)]^{1/2}$ value (a slight lowering of ν is compensated by a slight broadening of 3PA-transition) within the series of molecules studied. Therefore, disregarding a variation in $\nu^2/[g(0)]^{1/2}$ and substituting all the known values into (10), we obtain coherent domain sizes in each generation relatively to BDPAS. These results are shown in Fig 8 and Table 3. We see that, compared to BDPAS, the average domain size increases in 3SG0 and 4SG0 by ca. 14% and 32%, respectively. In 4SG1 the domain size becomes less, and in 4SG2 it drops back almost to the level of the parent compound. This behavior can be explained if we assume that lower-generation dendrimers are more planar, which facilitates the conjugation. The planarity may be lost in 4SG1 and 4SG2 [33], which can be seen as one reason for sudden decrease of the domain size.

We note that in our model all domains are assumed to be the same size. Of course, in reality, the size of the domains can vary inside one dendrimer. Such variation manifests itself, for example, in a difference of oscillator strengths of the split lowest 1PA transition obtained by quantum-chemical calculations (Table 3).

As the last step, we obtain the effective number of domains in each dendrimer by substituting the

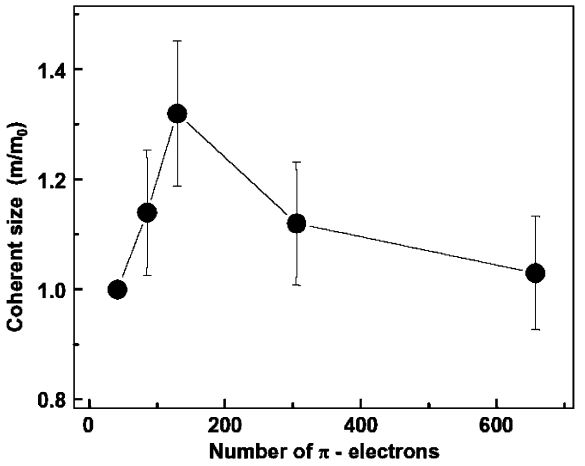

Fig. 8. Dependence of relative (to BDPAS) size of coherent domain on the number of π-electrons in BDPAS-based dendrimers.

above m/m_0 values into relation,

$$\mu = \frac{N_\pi}{N_{\pi,0}} \frac{m_0}{m}. \tag{11}$$

This gives for 3SG0, 4SG0, 4SG1, and 4SG2, respectively, $\mu = 1.9$, 2.4, 6.6, and 15.6. This result appears to be (at least for the first three molecules) in good correspondence with the number of low-lying singlet electronic transitions calculated by ZINDO/S method (Table 3).

Finally, we address an intriguing issue, what is the optimum size for a dendrimer, which would give the largest cooperative enhancement in 2PA and 3PA response? An answer to this question can be found when returning to Figs. 5 and 7. The plot shows that critical number of π-electrons appears to be around $N_\pi \sim 150$, above which the N_π^a dependence turns over into a linear one. Our conclusion is that this is likely the optimum size, which gives the best (per cost) performance of a π-conjugated dendrimer as an ultrafast two- and three-photon absorbing material.

4. Conclusions

In conclusion, we have studied two series of monodisperse dendrimers built of identical blocks of thriphenylamine-based chromophores BDPAS and BDPADSB. With both series we observe a strong cooperative enhancement effect in nonlinear 2PA and 3PA and show that it is due to the effective π-conjugation between constituent branches. For lower generation dendrimers, the peak 2PA cross section increases faster than linearly with the number of π-electrons. As compared to linear chain oligomers and polymers, the dendrimers are space-saving nanostructures, because their geometrical radius increases slower with the number of building blocks. Therefore, the demonstration of such cooperativity offers the possibility of large 2PA concentrated in extremely small (nanometer) volume, which can be used in a wide range of photonic applications. For the largest dendrimer, 4SG2, we have shown the largest absolute values of molecular 2PA- and 3PA cross section, with values, $\sigma_2 = 1.1 \times 10^{-46}\,\mathrm{cm^4\,s}$ and $\sigma_3 = 10^{-79}\,\mathrm{cm^6\,s^2}$, respectively. By comparing the 2PA cross section of the two dendrimer series, we conclude that by enlarging the conjugation system between the adjacent nitrogen atoms, even a low generation dendrimer such as 4BG0 can reach almost the same, remarkably large, σ_2 value as 4SG2. In practical terms, this means that considerably less synthesis work is needed to produce large 2PA cross section in dendrimers with BDPADSB branches.

We also have developed a new method of quantitative determination of the extent of conjugation described by the number and size of coherent domains by comparing 1PA and 3PA measurements. Coherent domain structure is deduced from 3PA measurements for all the dendrimers in one of the series. It is found that, in terms of largest coherence domain size, 4SG0 is the optimum dendrimer generation, which corresponds to an effective maximum number of conjugated π-electrons, $N_\pi \sim 150$. The described method of determining coherence domain size may be applicable also to other complex molecular nano-systems, such as J-aggregates, π-conjugated polymers, and others.

Acknowledgments

We thank Dr. A. Karotki, Dr. M. Kruk, and Dr. Y. Stepanenko for their help in experimental

measurements and Ms.Y. Dzenis for the help in performing quantum-mechanical calculations. This work was supported by AFOSR Grants F 49620-01-1-0406 and F 49620-01-1-0324.

References

[1] W. Denk, J.H. Strickler, W.W. Webb, Science 248 (1990) 73.
[2] W.R. Zipfel, R.M. Williams, W.W. Webb, Nat. Biotechnol. 21 (2003) 1369.
[3] J.D. Bhawalkar, N.D. Kumar, C.-F. Zhao, P.N. Prasad, J. Clin. Lasers Med. Surg. 15 (1997) 201.
[4] A. Karotki, M. Kruk, M. Drobizhev, A. Rebane, E. Nickel, C.W. Spangler, IEEE J. Sel. Top. Quantum Electron. 7 (2001) 971.
[5] B.H. Cumpston, S.P. Ananthavel, S. Barlow, D.L. Dyer, J.E. Ehrlich, L.L. Erskine, A.A. Heikal, S.M. Kuebler, I.-Y.S. Lee, D. McCord-Maughon, J. Qin, H. Röckel, M. Rumi, X.-L. Wu, S.R. Marder, J.W. Perry, Nature 398 (1999) 51.
[6] W.H. Zhou, S.M. Kuebler, K.L. Braun, T.Y. Yu, J.K. Cammack, C.K. Ober, J.W. Perry, S.R. Marder, Science 296 (2002) 1106.
[7] D.A. Parthenopoulos, P.M. Rentzepis, Science 245 (1989) 843.
[8] M. Albota, et al., Science 281 (1998) 1653.
[9] B.A. Reinhardt, et al., Chem. Mater. 10 (1998) 1863.
[10] C.W. Spangler, J. Mater. Chem. 9 (1999) 2013.
[11] J.E. Ehrlich, X.L. Wu, I.-Y.S. Lee, Z.-Y. Hu, H. Röckel, S.R. Marder, J.W. Perry, Opt. Lett. 22 (1997) 1843.
[12] M. Rumi, et al., J. Am. Chem. Soc. 122 (2000) 9500.
[13] Pond, S.J.K., Rumi, M., Levin, M.D., Parker, T.C., Beljonne, D., Day, M.W., Bredas, J.L., Perry, J.W., Marder, S.R. J. Phy. Chem. A 106 (2002) 11470.
[14] J.W. Perry, et al., Nonlinear Opt. 21 (1999) 225.
[15] L. Ventelon, L. Moreaux, J. Mertz, M. Blanchard-Desce, Chem. Commun. (1999) 2055.
[16] K.D. Belfield, et al., Org. Lett. 1 (1999) 1575.
[17] Z. Kotler, J. Segal, M. Sigalov, A. Ben-Asuly, V. Khodorkovsky, Synth. Met. 115 (2000) 269.
[18] S.-J. Chung, et al., Chem. Mater. 13 (2001) 4071.
[19] L. Ventelon, et al., Angew. Chem. Int. Ed. 40 (2001) 2098.
[20] O. Mongin, et al., Org. Lett. 4 (2002) 719.
[21] M. Blanchard-Desce, C.R. Physique 3 (2002) 439.
[22] A. Abbotto, et al., Org. Lett. 4 (2002) 1495.
[23] B. Strehmel, A.M. Sarker, H. Detert, Chem. Phys. Chem. 4 (2003) 249.
[24] T.-C. Lin, G.S. He, P.N. Prasad, L.-S. Tan, J. Mater. Chem. 14 (2004) 982.
[25] B. Paci, C. Andraud, R. Anemian, J.-M. Nunzi, J. Phys. B: At. Mol. Opt. Phys. 37 (2004) 1581.
[26] R. Kopelman, et al., Phys. Rev. Lett. 78 (1997) 1239.
[27] M. Halim, J.N.G. Pillow, I.D.F. Samuel, P.L. Burn, Adv. Mater. 11 (1999) 371.
[28] R.G. Ispasoiu, et al., J. Am. Chem. Soc. 122 (2000) 11005.
[29] K. Ashworth, et al., Abstr. Pap. Am. Chem. Soc. 219 (Part 2) (2000) 423.
[30] O. Mongin, J. Brunel, L. Porrès, M. Blanchard-Desce, Tetrahedron Lett. 44 (2003) 2813.
[31] S.-J. Chung, et al., J. Phys. Chem. B 103 (1999) 10741.
[32] M. Drobizhev, A. Karotki, A. Rebane, C.W. Spangler, Opt. Lett. 26 (2001) 1081.
[33] M. Drobizhev, et al., J. Phys. Chem. B 107 (2003) 7540.
[34] J. Yoo, S.K. Yang, M.Y. Jeong, H.C. Ahn, S.J. Jeon, B.R. Cho, Org. Lett. 5 (2003) 645.
[35] M. Drobizhev, et al., J. Phys. Chem. B 108 (2004) 4221.
[36] A. Abbotto, et al., Chem. Commun. (2003) 2144.
[37] S.A. Lahankar, et al., J. Chem. Phys. 120 (2004) 337.
[38] A. Karotki, Simultaneous two-photon absorption of tetrapyrrolic molecules: from femtosecond coherence experiments to photodynamic therapy, Ph.D. Thesis, Montana State University, 2003. 〈http://www.montana.edu/etd/available/karotki_03.html〉.
[39] C.W. Spangler, et al., Mater. Res. Soc. Symp. Proc. 597 (2000) 339.
[40] E.H. Elandaloussi, et al., Mater. Res. Soc. Symp. Proc. 597 (2000) 344.
[41] Z.Y. Suo, et al., Abstr. Pap. Am. Chem. Soc. 226 (Part 2) (2003) 422.
[42] M. Drobizhev, et al., Chem. Phys. Lett. 325 (2000) 375.
[43] A.N. Sobolev, et al., Acta Cryst. C 41 (1985) 967.
[44] X. Wang, et al., J. Mater. Chem. 11 (2001) 1600.
[45] R. Sander, et al., Macromolecules 29 (1996) 7705.
[46] G. Yu, et al., Appl. Phys. Lett. 74 (1999) 2295.
[47] J.M. Lupton, et al., J. Phys. Chem. B 106 (2002) 7647.
[48] J.-S. Yang, S.-Y. Chiou, K.-L. Liau, J. Amer. Chem. Soc. 124 (2002) 2518.
[49] J. Swiatkiewicz, P.N. Prasad, B.A. Reinhardt, Opt. Commun. 157 (1998) 135.
[50] P. Macak, Y. Lou, H. Norman, H. Agren, J. Chem. Phys. 113 (2000) 7055.
[51] N.S. Bayliss, J. Chem. Phys. 16 (1948) 287.
[52] R. Anemian, P.L. Baldeck, C. Andraud, Mol. Cryst. Liq. Cryst. 374 (2002) 335.
[53] P. Norman, Y. Luo, H. Ågren, Chem. Phys. Lett. 296 (1998) 8.
[54] P. Norman, Y. Luo, H. Ågren, Opt. Commun. 168 (1999) 297.
[55] X. Zhou, et al., J. Mol. Struct. 672 (2004) 175.
[56] M.G. Kuzyk, J. Chem. Phys. 119 (2003) 8327.
[57] A.C. Selden, Nature Phys. Sci. 229 (1970) 210.
[58] R. Pantell, F. Pradere, J. Hanus, M. Schott, H. Puthoff, J. Chem. Phys. 46 (1967) 3507.
[59] C. Xu, W. Zipfel, J.B. Shear, R.M. Williams, W.W. Webb, Proc. Natl. Acad. Sci. USA 93 (1996) 10763.
[60] S. Maiti, J.B. Shear, R.M. Williams, W.R. Zipfel, W.W. Webb, Science 275 (1997) 530.